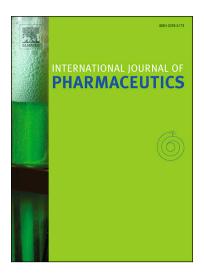
pH-responsive Chimeric Liposomes: From Nanotechnology to Biological Assessment

Nikolaos Naziris, Francesca Saitta, Varvara Chrysostomou, Marcin Libera, Barbara Trzebicka, Dimitrios Fessas, Stergios Pispas, Costas Demetzos

PII:	S0378-5173(19)30894-4
DOI:	https://doi.org/10.1016/j.ijpharm.2019.118849
Reference:	IJP 118849
To appear in:	International Journal of Pharmaceutics
Received Date:	4 July 2019
Revised Date:	2 November 2019
Accepted Date:	4 November 2019



Please cite this article as: N. Naziris, F. Saitta, V. Chrysostomou, M. Libera, B. Trzebicka, D. Fessas, S. Pispas, C. Demetzos, pH-responsive Chimeric Liposomes: From Nanotechnology to Biological Assessment, *International Journal of Pharmaceutics* (2019), doi: https://doi.org/10.1016/j.ijpharm.2019.118849

This is a PDF file of an article that has undergone enhancements after acceptance, such as the addition of a cover page and metadata, and formatting for readability, but it is not yet the definitive version of record. This version will undergo additional copyediting, typesetting and review before it is published in its final form, but we are providing this version to give early visibility of the article. Please note that, during the production process, errors may be discovered which could affect the content, and all legal disclaimers that apply to the journal pertain.

© 2019 Published by Elsevier B.V.

pH-responsive Chimeric Liposomes: From Nanotechnology to Biological Assessment Nikolaos Naziris^{a,niknaz@pharm.uoa.gr}, Francesca Saitta^{b,francesca.saitta@unimi.it,sereti_e@yahoo.gr}, Varvara Chrysostomou^{c,chrisostomou.varvara@gmail.com}, Marcin Libera^{d,marcin.libera77@gmail.com}, Barbara Trzebicka^{d,btrzebicka@cmpw-pan.edu.pl}, Dimitrios Fessas^{b,dimitrios.fessas@unimi.it}, Stergios Pispas^{c,pispas@eie.gr}, Costas Demetzos^{a,*,demetzos@pharm.uoa.gr,ksdimas@yahoo.com}

^aSection of Pharmaceutical Technology, Department of Pharmacy, School of Health Sciences, National and Kapodistrian University of Athens, Panepistimioupolis Zografou, Athens, 15771, Greece

^bDepartment of Food, Environmental and Nutritional Sciences (DeFENS), Università degli Studi di Milano, Via Celoria 2, Milano, 20133, Italy

^cTheoretical and Physical Chemistry Institute, National Hellenic Research Foundation, 48 Vassileos Constantinou Avenue, Athens, 11635, Greece

^dCentre of Polymer and Carbon Materials, Polish Academy of Sciences, Zabrze, Poland

*Corresponding author.

Graphical abstract

Abstract

The utilization of liposomes in biomedical applications has greatly benefited the diagnosis and treatment of various diseases. These biomimetic nano-entities have been very useful in the clinical practice as drug delivery systems in their conventional form, comprising lipids as structural components. However, the scientific efforts have recently shifted towards the development of more sophisticated nanotechnological platforms, which apply functional biomaterials, such as stimuli-responsive polymers, in order to aid the drug molecule targeting concept. These nanosystems are defined as

chimeric/mixed, because they combine more than one different in nature biomaterials their development requires intensive study through biophysical and and thermodynamic approaches before they may reach *in vivo* application. Herein, we designed and developed chimeric liposomes, composed of a phospholipid and pHresponsive amphiphilic diblock copolymers and studied their morphology and their behavior based on crucial formulation parameters, including biomaterial concentration, dispersion medium pH and polymer composition. Additionally, their interactions with biological components, pH-responsiveness and membrane thermodynamics were also assessed. Finally, preliminary in vivo toxicity experiments of the developed nanosystems were carried out, in order to establish a future protocol for full in vivo evaluation. The results have been correlated with the properties of the chimeric nanosystems and highlight the importance of such approaches for designing and developing effective nanocarriers for biomedical applications.

Keywords: Chimeric liposomes; pH-responsive; lyotropism; interactions; micro-DSC **Abbreviations:** aDDnSs, Advanced drug delivery nanosystems; Cryo-TEM, Cryogenic transmission electron microscopy; DDnSs, Drug delivery nanosystems; DLS, Dynamic light scattering; ELS, Electrophoretic light scattering; FBS, Fetal bovine serum; HSPC, L-a-phosphatidylcholine, hydrogenated (soy); Micro-DSC, Micro-differential scanning calorimetry; MLV, Multilamellar vesicle; PBS, Phosphate buffer saline; PDMAEMA-b-PLMA, Poly(2-(dimethylamino)ethyl methacrylate)-bpoly(lauryl methacrylate); SUV, Small unilamellar vesicle

1. Introduction

Nanomedicine is the interdisciplinary field where nanoscience and nanotechnology converge with life sciences. This approach is present in everyday clinical practice and provides applications related to drug delivery, diagnostic and imaging tools, implants and many more (Pelaz et al., 2017). Regardless of the application, the most important and useful tools of Nanomedicine are nanoparticles, which suggest a wide field of manufactured organic and inorganic systems, amongst them being lipidic nanosystems, such as liposomes (Akbarzadeh et al., 2013) and micelles (Torchilin, 2007), polymeric nanoparticles, for example micelles (Zhang et al., 2014), dendrimers (Palmerston et al., 2017) and polymersomes (Zhang et al., 2014), carbon nanomaterials, like nanotubes (Baughman et al., 2002), grapheme (Nurunabi et al., 2014) and nanodiamonds (Yu et al., 2005), mesoporous silica nanoparticles (Bharti et al., 2015), quantum dots (Parak et al., 2005), gold nanoparticles (Lin et al., 2009), superparamagnetic iron oxide nanoparticles (Colombo et al., 2012) etc. The everbranching discovery of nanomaterials and synthesis of nanosystems from these materials has rendered their classification a difficult task and many efforts and propositions have been made to this end, hence the terms non-biological complex drugs (NBCDs), conventional and advanced drug delivery nanosystems (cDDnSs and aDDnSs) and many other approaches (Schellekens et al., 2014; Demetzos and Pippa, 2014). These classifications are usually accompanied by respective propositions on the regulation of nanomedicinal products.

Nanoparticles should fulfill certain criteria, in order to have a chance to succeed in delivering their payload inside biological environment. Those include physical stability, stealth behavior and biological stability, prolonged circulation, tissue targeting, cellular targeting, cellular uptake and intracellular spatiotemporal release (Lehner et al., 2013). The rationale for successful drug delivery and targeting further

involves the utilization and combination of many different and diverse mechanisms, all of which obey to one or both of the following general phenomena: passive or active targeting of tissues. Passive targeting is the basic principle that governs the nanoscale, depending on the well-known phenomenon of the enhanced permeability and retention (EPR) effect and serving the accumulation of very small particles inside the rapidly growing tumor tissues (Maeda, 2001). Active targeting design utilizes very specific particle-target cell interactions, through attachment of ligands on the surface of nanocarriers that will bind on overly expressed receptors on the surface of the target cells (Danhier et al., 2010). Following the targeting step, the nanocarriers are destined to release their cargo to the extracellular microenvironment, e.g. via the stimuli-responsiveness mechanism, or enter the cell, again through one or more pathways, including passive diffusion through the cell membrane, endocytic cellular uptake (Doherty and McMahon, 2009), cellular uptake by cell-penetrating peptides (Frankel and Pabo, 1988). Of course, active targeting through ligand-receptor binding is a route which might also lead to endocytosis. Finally, intracellular release of drugs occurs after endosomal escape, for example by exploiting the mildly acidic environment of these organelles through pH-responsiveness (Gunther et al., 2011; Naziris et al., 2016).

Liposomes have long been in the market as DDnSs, primarily of drug molecules that are indicated for cancer or infectious diseases (Bulbake et al., 2017b). Since the marketing of the first FDA-approved nano-drug, Doxil®, a lot of effort has been placed on the development of more sophisticated formulations, which will go beyond the secured concepts of stability, prolonged circulation and passive accumulation on the disease site of the nanocarriers (Barenholz, 2012). In this context, the integration of polymeric technology on the liposomal platform has led to the implementation of a

new field of applications, where the versatile polymer synthesis meets the dynamic self-assembly of membranes and together they build innovative structures with new morphologies and functionalities (Schulz and Binder, 2015; Naziris et al., 2017). These aDDnSs have been assigned the terms "mixed", "hybrid" or "chimeric" vesicles and liposomes (Demetzos and Pippa, 2014).

Stimuli-responsive biomaterials and drug delivery nanosystems are components of next-generation therapeutics, with hallmarks that surpass the conventional technologies and their investigation has provided a substantial contribution to the field of Nanomedicine. This innovative class suggests nanocarriers which are able to respond to well-defined internal/intrinsic stimuli that are present in pathological sites, including alterations in pH, temperature, redox conditions and biomolecule/enzyme expression or extrinsic/external ones, including heat, magnetic field, light and ultrasounds (Deshpande et al., 2013; Naziris et al., 2016). Currently, there are a few nanotechnological formulations that implement the stimuli-responsive concept under clinical trial. However, only the thermosensitive liposomes of Thermodox® have succeeded in reaching an advanced clinical stage, currently on Phase III for breast cancer (Anselmo and Mitragotri, 2016). This product comprises DPPC, MPPC and DSPE-PEG 2000 and its thermosensitivity depends on the responsiveness of the lysolipid to high temperature (~42°C), provided by externally applied microwave hypothermia, ultrasound, or radiofrequency thermal ablation (Eloy et al., 2014). In parallel, pH-responsive nanosystems have also been extensively and thoroughly studied, among others via the combination of liposomal platform with pH-responsive polymeric molecules, for the development of chimeric/mixed functional nanocarriers (Felber et al., 2012; Kanamala et al., 2016). Despite that fact, a successful clinical application still remains to be seen from this effort.

The purpose of the present study was to develop pH-responsive chimeric/mixed liposomes and to study and evaluate their lyotropism/lyotropic behavior, based on their concentration-dependent self-assembly process (Naziris et al., 2018). In addition, the morphology and the behavior of liposomes under various environmental conditions, *i.e.* acidic pH and protein binding, as well as their size, polydispersity and zeta potential alterations were also evaluated. Micro-DSC was utilized as means to evaluate the thermotropic behavior of the liposomes in normal and acidic conditions, as well as their stability. Finally, preliminary in vivo experiments provided an estimation on which nanosystems are best candidates for further evaluation. Chimeric liposomes were composed of the phospholipid HSPC (Figure 1A) and of the pHresponsive amphiphilic diblock copolymers PDMAEMA-b-PLMA 1 and 2 (Figure **1B**). The phospholipid is a common ingredient among liposomal products, exhibiting high main phase transition temperature from the gel phase to the liquid crystalline phase, *i.e.* ~53.6°C and a very low-enthalpy pre-transition (Kitayama et al., 2014). This polymer responds to thermal and pH alterations, depending on its composition and molecular weight, both attributed to the PDMAEMA segment (Samsonova et al., 2011; Zengin et al., 2013). As a result, it has been utilized to build functional nanocarriers, either polymeric or chimeric ones, e.g. by incorporation inside lipid bilayers through the PLMA hydrophobic block (Figure 1C) (Chrysostomou and Pispas, 2018; Naziris et al., 2018).

2. Materials and methods

2.1. Materials

The phospholipid HSPC, with molecular weight (M_w) of 783.774, was purchased from Avanti® Polar Lipids, Inc. (Alabaster, AL, USA) and used without further purification (**Figure 1A**). Chloroform, methanol and other reagents were of analytical grade and purchased from Sigma-Aldrich® Co. FBS was Gibco® and purchased from Thermo Fisher Scientific. The PDMAEMA-b-PLMA amphiphilic diblock copolymers were synthesized by RAFT polymerization methodologies, in two different molar compositions, 70-30 for PDMAEMA-b-PLMA 1 and 58-42 for PDMAEMA-b-PLMA 2 (**Figure 1B**). The M_w of the copolymers, determined by size exclusion chromatography (SEC), equals 8,900 and 10,800 respectively. The copolymer synthesis has been presented thoroughly in our previous publication (Naziris et al., 2018).

2.2. Preparation of Pure and Chimeric Vesicles

Chimeric liposomal systems of HSPC and HSPC:PDMAEMA-b-PLMA 1/2 have been prepared, by utilizing the thin-film hydration method. Specifically, appropriate amounts of HSPC and PDMAEMA-b-PLMA 1/2 (9:0.1 and 9:0.5 molar ratios) were dissolved in chloroform and chloroform/methanol (9:1 v/v) respectively and then transferred into a round flask, connected to a rotary evaporator (Rotavapor R-114, Buchi, Switzerland). Vacuum was applied and the chimeric phospholipid/block copolymer thin film was formed by slow removal of the solvent at 40°C. The mixed film was maintained under vacuum for at least 24h in a desiccator, in order to remove possible traces of solvent. Afterward, it was hydrated with PBS 150mM (pH = 7.0 for micro-DSC or 7.4 for *in vivo* toxicity), by slowly stirring for 1h in a water bath, above the phase transition temperature of the lipid (~52°C for HSPC). The final total concentration of the formulations 5mg/mL for micro-DSC and 20 and 40mg/mL for *in vivo* experiments. The resultant particles (apparently MLVs) were subjected to two 5min sonication cycles (amplitude 70%, cycle 0.5sec) interrupted by a 5min resting period, by using a probe sonicator (UP 200S, dr. Hielsher GmbH, Berlin, Germany), in order to produce nanoparticles (tentatively assigned as small unilamellar vesicles, SUVs), which were allowed to anneal for 30min.

2.3. Light Scattering Techniques

The size, size distribution and zeta potential of the obtained liposomes were investigated by DLS and ELS, respectively. The physicochemical characteristics were measured immediately after preparation (t = 0days), as well as over a 30-day period, to monitor the colloidal system physical stability. For DLS and ELS, aliquots were diluted in HPLC-grade water, 30-fold for the lowest concentration and 60-fold for the higher ones, in order to always obtain clear samples. In addition, acidic protocol was performed, by 10-fold diluting samples in citrate buffer 100mM (pH = 4.5), allowing them to anneal for 15 to 20mins and then 3 or 6-fold diluting them in HPLC-grade water. Furthermore, 5mg/mL samples were 30-fold diluted in FBS, in order to assess the liposome-protein interactions. Measurements were performed at a detection angle of 90° and at 25°C, in a photon correlation spectrometer (Zetasizer 3000 HSA, Malvern, UK) and analyzed by the CONTIN method (MALVERN software). Details on the methods have been published elsewhere (Pippa et al., 2014).

2.4. Cryo-TEM

Cryo-TEM micrographs were obtained using a Tecnai F20 TWIN microscope (FEI Company, USA), equipped with field emission gun, operating at an acceleration voltage of 200kV. Images were recorded on the Eagle 4k HS camera (FEI Company, USA) and processed with TIA software (FEI Company, USA). Specimens for investigation were prepared through vitrification by plunge freezing of the aqueous

suspensions on copper grids (300mesh) with holey carbon film (Quantifoil R 2/2; Quantifoil Micro Tools GmbH, Germany). Prior to use, the grids were activated for 30s in oxygen plasma using a Femto plasma cleaner (Diener Electronic, Germany). The suspension of sample (2.1µL) was put drop onto grid, next blotted using dedicated filter paper and immediately frozen by plunging in liquid ethane, utilizing a fully automated and environmental controlling blotting device Vitrobot Mark IV (FEI Company, USA). Specimens after vitrification were kept under liquid nitrogen until they were inserted into a cryo-TEM-holder Gatan 626 (Gatan Inc., USA) and analyzed in the TEM at -178°C. Pictures were processed using ImageJ software.

2.5. Micro-DSC

Thermal analysis was employed to assess the composition and concentrationdependent effect of the two different block copolymers on the stability of the chimeric liposomes, with respect to their gel-to-liquid crystal phase transition. The measurements were accomplished by using a Setaram micro-DSCIII (Setaram Instrumentation, Caluire, France), operating with 1mL hermetically closed pans, at 0.5° C/min scanning rate. The pure HSPC and chimeric liposomal suspensions in PBS 150mM (pH = 7.0) were diluted up to 2.5mg/mL concentration, referred to the overall weight. The dilution was achieved by adding PBS 150mM (pH = 7.4) or citrate buffer 100mM (pH = 4.5). Instead, classic DSC technique was selected to obtain thermograms for HSPC MLVs as reference, apart from SUVs, showing the lipid transition from the planar-gel to the liquid-crystal phases. A PerkinElmer DSC6 (PerkinElmer, Waltham, MA, USA), working with hermetically closed pans, was used at 0.5°C/min scanning rate. MLV samples were prepared with a 0.2mg/mL lipid concentration. For all the experiments, two heating-cooling cycles were scheduled and the second cycle was considered as thermodynamically meaningful, in order to

10

evaluate the properties of the chimeric systems. The raw data were analyzed through appropriate software, THESEUS (Barone et al., 1992). Thermograms were expressed in terms of excess specific heat, C_p^{exc} , with respect to the low temperature lipid state, by adjusting the baseline and the relevant thermodynamic parameters, *i.e.* the transition enthalpy ΔH , main transition temperature T_m and relative transition (full width at half maximum) $\Delta T_{1/2}$, were calculated. Specifically, apparent transition temperatures were indicated as $T_{m,l}^{app}$ and $T_{m,2}^{app}$ in the cases of biphasic traces and were used to describe the overall stability of a particular thermodynamic phase, compared to the reference system. Moreover, the relative transition $\Delta_r T_{1/2}$ expresses a cooperativity comparison parameter, defined as $\Delta_r T_{1/2} = \Delta T_{1/2}$ (system) / $\Delta T_{1/2}$ (pure MLVs), making the pure MLVs' $\Delta T_{1/2}$ as the reference value for the full width at half maximum of each peak.

2.6. In vivo Experiments

For the preliminary *in vivo* toxicity study, NOD.CB17-*Prkdc^{scid}*/J mice, purchased from Jackson Laboratory (The Jackson Laboratory 600 Main Street Bar Harbor, Maine 04609 USA), were utilized. The mouse colony was maintained in a pathogen-free environment in type IIL cages. Male mice, 6-8 weeks old, were used in the studies described here. All animals were kept under specific pathogen free (SPF) conditions at the animal facility the Department of Pharmacology, EL42-BIO_Exp03, in a climate-regulated environment (21± 1C; 50-55% relative humidity), under a 12h/12h (lights on at 7:00 AM) and allowed *ad libitum* food and water. Toxicity experiments were performed following the guidelines of the USA National Cancer Institute ("National Cancer Institute", 2015; Iatrou et al., 2014). Chimeric liposomes were administered intraperitoneally (i.p.) in the lateral aspect of the lower left quadrant. Handling and experimentation of animals were according to Greek laws

(2015/92) and the guidelines of the European Union and European Council (86/609 and ETS123, respectively).

2.7. Statistical Analysis

DLS and ELS results are shown as mean value ± standard deviation (SD) of three independent measurement means. Statistical analysis was performed using Student's t-test and multiple comparisons were done using one-way ANOVA. P-values < 0.05 were considered statistically significant. All statistical analyses were performed using "Microsoft Office EXCELL".

3. Results and discussion

3.1. Lyotropism and Physicochemical Characteristics of Chimeric Liposomes

The physicochemical characteristics of the developed chimeric liposomal systems are presented in **Table 1** and **2**, while cryo-TEM images are provided in **Figure 2**. In **Table 1** are presented the liposomal formulations utilized for micro-DSC experiments, developed at a total biomaterial concentration, *i.e.* lipid and polymer combined, of 5mg/mL, while **Table 2** includes the liposomes developed for *in vivo* experiments, in 20mg/mL and 40mg/mL biomaterial concentrations. The reason for this approach is that *in vivo* experiments may require a high amount of nanocarriers, in order to achieve sufficient amount of a drug molecule for a dose scheme that is intended for therapeutic applications. As a result, toxicity studies should ensure that even at a very high administrated concentration, nanocarriers will be non-toxic. This will further ensure that the therapeutic concentration of nanocarriers, defined by the therapeutic dose of drug molecule, will also be non-toxic (Abra et al., 1980). Under the experimental conditions used herein, we observed that there were some

differences between the three utilized concentrations, concerning the size of some chimeric nanosystems exceeding the 100nm threshold when developed at higher concentration. An important factor in this is also the slight pH alteration from 7.0 to 7.4, the effect of which is discussed below. Apart from that, the ζ -potential, was measured to be high in value for high-concentration formulations of 9:0.1 molar ratio. This might be attributed to the formation of different types of morphologies between 9:0.1 and 9:0.5 formulations of 20mg/mL or 40mg/mL biomaterial concentration and the consequent exposure of positively charged amino groups towards the environment in different ways (Naziris et al., 2017).

An essential aspect of lyotropic liquid crystalline systems, besides the total biomaterial concentration, is their composition. In our study, liposomes are comprised of a well-established phospholipid, component of marketed liposomal products, among which the first to be authorized, Doxil®, as well as of an amphiphilic diblock copolymer, belonging to the stimuli-responsive class (Bulbake et al., 2017). The latter was also synthesized in two different molar compositions, 70-30 for PDMAEMA-b-PLMA 1 and 58-42 for PDMAEMA-b-PLMA 2. Since the PDMAEMA groups are generally hydrophilic, if kept below the LCST (approx. 40-50°C) and below the pK_a value of the amino groups (approx. 7.5-8.0), while the PLMA groups are always hydrophobic, the PDMAEMA-b-PLMA 1 copolymer has a more hydrophilic balance at certain conditions (Samsonova et al., 2011; Zengin et al., 2013). The lyotropic effect of the polymer hydrophilic-to-hydrophobic balance, as well as of its molar ratio inside the chimeric system has been thoroughly studied in terms of morphological variety and biophysical impact *in vitro* (Naziris et al., 2017; Naziris et al., 2018).

Another parameter affecting the lyotropism of liquid crystalline systems, such as liposomes, is the environmental pH, especially for chimeric nanosystems with pH-

responsive components. In all cases, formulations were built inside PBS, however, the pH of the medium was slightly more acidic than the physiological, in the case of 5mg/mL, in order to compare the self-assembly process with that of our previous investigation. Specifically, this allowed for evaluation of the ionization degree effect of PDMAEMA on the self-assembly and final properties of nanoassemblies. More specifically, the amino groups of PDMAEMA become more protonated as the medium pH decreases and this gradient ionization apparently promotes the insertion of the copolymer inside the phospholipid bilayer in different ways. This is evident if we compare the results of Table 1 with that from previous studies (Naziris et al., 2018). The chimeric liposomes in the present study are smaller in size and more homogeneous in particle distribution, reflected in the D_h and PDI values respectively. Their zeta potential however, is not particularly different than before, if we take into account the standard deviation, something that at first impression contradicts the increased ionization of the polymer. Probably the observed behavior is due to the amino groups being hidden from the hydrophilic surface formed by the extended polymer chains, resulting in a surface charge that is not much different if the groups near the bilayer are more positively charged. The approach of altering the pH to improve the self-assembly of chimeric liposomes could be a part of formulation optimization conditions for such lyotropic systems.

Concerning the effect of the polymer on the final liposomal physicochemical characteristics, we observe that all chimeric systems are in the nanoscale, around 30nm smaller than conventional HSPC liposomes and they are all very homogeneous, with polydispersity values ranging between 0.20 and 0.28. The cryo-TEM visualization confirms the existence of vesicular morphologies with uniform size distribution of the sample species formed in aqueous medium (**Figure 2**). The surface

charge of chimeric liposomes is also considerably more positive than neat liposomes, owing to the positively charged amino groups of the anchored PDMAEMA chains in this pH, indicating the incorporation of the copolymer inside the liposomal membrane. Nevertheless, the effect of the composition and concentration of the copolymer on the size, homogeneity and surface charge of the systems is not profound in these preparation conditions, even though the two copolymers have different hydrophilic-to-hydrophobic balance and five-times more polymer has occasionally been utilized. It is evident that under these lyotropic conditions, chimeric nanocarriers with different type and amount of polymer may be built, with adequate physicochemical characteristics for future applications. As a result, we propose that certain parameters, including medium pH, may considerably affect the creation of nanomorphologies, possibly averting the formation of non-vesicular morphologies (Naziris et al., 2017). In this way, optimum conditions for chimeric liposomal development may be defined for individual nanosystems of specific biomaterials, *e.g.* phospholipid and pH-responsive amphiphilic polymer.

In addition, these nanosystems are stable in due time, in terms of particle size (**Figure S1**), because of the steric and electrostatic repulsion provided by the water-soluble PDMAEMA polymer segments, but also because of the lyotropic effect that the PLMA segments have on the membrane, which is presented below in the micro-DSC section. The polydispersity was stable for both the conventional and the chimeric nanosystems (**Figure S2**). The colloidal stability is also an indication of the incorporation of the polymer inside the lipid membrane.

3.2. The pH-responsiveness and Protein Interactions of Chimeric Liposomes

Chimeric nanosystems provide a plethora of benefits inside the field of drug delivery, mainly by enabling the bio-functionalization of conventional nanocarriers with synthetic biomaterial, such as dendrimers or polymers. One of many concepts is to render liposomes responsive to physiological stimuli, in this case pH alterations. In this way, they exist inside the circulation (pH = 7.4) in an equilibrium state, while they undergo transition when they meet the tumor, endosomal or lysosomal environment, with pH values around 5.7-7.0, 5.0-6.5 and 4.5-5.0 respectively. The pathway by which this may happen includes many different mechanisms (Felber et al., 2012).

Regarding their behavior in acidic pH environment (pH = 4.5), the chimeric nanocarriers were not affected much in terms of size and homogeneity (Table 1). This means that the copolymer response to pH fluctuations and its subsequent conformation alteration is not enough to significantly alter the membrane physicochemical characteristics. In our previous investigation, the size of particles was found smaller in acidic conditions, compared with normal. However, this was attributed to possible electrostatic repulsion and hydration forces that probably separated vesicles that were close to each other, while here liposomes were already far from each other, due to more acidic formulation medium (pH = 7.0 vs. 7.4), reflected on the considerably smaller size they exhibited after preparation (Naziris et al., 2018). In addition, the zeta potential was found slightly increased in acidic pH, owed to the PDMAEMA chains being more positively charged in these conditions ($pK_a = 7.5-8.0$) (Samsonova et al., 2011; Zengin et al., 2013). Nevertheless, these pH-responsive chimeric liposomes can be utilized not only to carry drug molecules inside their hydrophilic core or hydrophobic bilayer, but also through complexation of the therapeutic molecule (nucleic acid, drug or protein) with the extended and positively

charged hydrophilic polymer chains. The presence of positively charged PDMAEMA chains may also allow for the complexation of targeting moieties through electrostatic interactions (Zhu et al., 2010).

Incubation in protein-containing medium is of primary importance to test the biological stability of DDnSs, especially for those that expose a charged surface to the outer environment. FBS mainly contains bovine serum albumin (BSA) that has a negative effective charge in physiological pH, close to -10mv, and is expected to approach positively charged nanoparticles and bind on their surface electrostatically, altering their physicochemical properties, *i.e.* their hydrodynamic diameter, zeta potential and polydispersity index (Böhme and Scheler, 2017; Papageorgiou et al., 2018).

The interactions of the chimeric liposomes with FBS are presented in **Table 1**. The increase in particle size is evident, since all nanosystems had their size increased from around 80nm, to up to 190nm, indicating the formation of a "protein corona". However, this increase is something expected, due to the charged nature of these nanoparticles and is not considered that important. Furthermore, the polydispersity of all systems is maximum or close to maximum, indicating that the size distribution is heterogeneous in all cases, also expected due to serum-originated aggregation (Mohr et al., 2014, Pippa et al., 2016). What is more, a varying behavior among the four chimeric nanosystems is observed. It is a result of the nature of the utilized amphiphilic copolymer, of which the hydrophilic-to-hydrophobic balance directly affects the protein-nanocarrier interactions. Evidently, the more hydrophilic macromolecule induces these interactions, since it provides liposomes with larger positively charged hydrophilic corona, while the hydrophobic one makes liposomes stealthier. Interestingly, this finding may contribute to the design of a roadmap for

optimum chimeric formulations, where the composition and concentration of incorporated macromolecules and, consequently, their lyotropic effect on the liposomal membrane will be decided based on the balance between physicochemical properties, physical stability and biological stability, namely protein interactions thereof. It should also be noted that the utilized protocol for protein interactions exposes the nanosystems to high amount of proteins (100 μ L of liposomes were diluted with 2900 μ L FBS), compared with other studies (1:1 sample to FBS dilution) (Palchetti et al., 2016a).

The zeta potential of the nanocarriers diluted in FBS could not be assessed, because of the existence of aggregates in the samples. As a result, only the measured size holds essential value and it is obvious that the serum proteins are adhered onto the chimeric liposomes' surface through electrostatic interactions and lead to opsonization and finally protein corona formation. This finding should be taken into account for both *in* vitro and in vivo biological applications, though protein type and abundance differ between the two models, as well as between animals and humans (Zeitlinger et al., 2011). In particular, the protein corona that was observed for all chimeric nanosystems is expected to affect the mechanism and degree of cellular uptake of nanoparticles during in vitro investigations (Palchetti et al., 2016b). In addition, immune cell recognition, clearance and off-target interactions are some of the main issues that will determine the final *in vivo* toxicity and targeting effectiveness of these nanosystems. In some cases, the protein corona might favorably affect nanoparticlecell interactions, association and final cellular uptake. The protein corona layer is the main feature of surface recognition in physiological environment and is considered a "biological fingerprint" for nanoparticles, depending on their composing biomaterials,

as well as on the self-assembly process between them that gives rise to certain morphologies and surface properties (Palchetti et al., 2019).

3.3. Thermodynamic Stability of Chimeric Liposomes

In order to evaluate the thermodynamics and stability of liposomes, calorimetric experiments need to be performed on liposomal suspensions of low concentration, *e.g.* 5mg/mL in PBS. For this reason, we selected the micro-DSC as the most suitable technique, in terms of sensitivity, and diluted the formulations to 2.5mg.mL, to study the composition- and concentration-dependent thermotropic effect of the utilized copolymers on HSPC membranes (Gardikis et al., 2010). Thermograms obtained for the investigated systems are shown in **Figure 3** to **5** and the relevant thermodynamic parameters, *i.e.* ΔH , T_m and $\Delta_r T_{1/2}$, are reported in **Table 3**.

In **Figure 3**, a comparison between pure HSPC bilayers/MLVs and liposomes/SUVs is reported, to highlight the differences in the main phase transition, depending on the geometry of the membrane (Saitta et al., 2019). In the case of the HSPC MLVs (blue curve), we observed the typical pre-transition peak (at about 48.2°C) followed by the main gel-to-liquid crystal transition ($T_m = 53.8^{\circ}$ C), with a narrow $\Delta T_{1/2}$ (0.75°C), which reflects the high cooperativity. Such $\Delta T_{1/2}$ was used as reference breadth value for the $\Delta_r T_{1/2}$ estimation for each system. A typical thermogram for liposomal systems is also observed in the case of HSPC liposomes (black curve), *i.e.* a broad peak ($\Delta_r T_{1/2} = 4.4$), apparently not preceded by a pre-transition. Furthermore, the thermogram is characterized by a biphasic behavior, in line with the fact that HSPC consists of a mixture of two different phospholipids. In spite of the cooperativity differences, the overall transition enthalpy was very close to those of MLVs. We observed that the MLVs' T_m is in agreement with the high temperature apparent maximum (shoulder) of

liposomes, indicating the prevalence of thermodynamically more stable phases in MLVs, as expected (Koynova and Caffrey, 1998; Kitayama et al., 2014).

Micro-DSC scans for both HSPC:PDMAEMA-b-PLMA 1 and HSPC:PDMAEMA-b-PLMA 2 chimeric systems in PBS 150mM (pH = 7.4) and citrate buffer 100mM (pH= 4.5) are shown in Figure 4, including the pure HSPC liposomes as reference (black curve). Concerning PBS, both chimeric systems exhibited a behavior which was totally reversible, similarly to the pure system, and also strongly dependent on copolymer concentration. As for the liposomes' thermodynamic stability at low copolymer concentration 9:0.1 (red curves), these nanosystems were slightly stabilized and the entropic contribution seemed to be dominant. Indeed, the thermograms were shifted few Celsius degrees (1 to 2°C) towards higher temperature values, whereas the overall enthalpy for the gel-to-liquid crystalline transition was nearly the same for each investigated system, compared with the reference (ΔH° = 40±2kJ·mol⁻¹). The variations in the thermodynamic profiles confirmed the interaction and the insertion of the PLMA chains within the liposome's hydrophobic core, whereas the enthalpic contribution due to the impairment of phospholipidphospholipid interactions might be too small to be detected for so low copolymer concentrations. Besides these general similarities, different effects of the two copolymers on the stability of the several thermodynamic phases were observed. In the case of the HSPC:PDMAEMA-b-PLMA 1 9:0.1 system, the overall copolymerinduced stabilization was accompanied by a slight cooperativity decrease, while maintaining the same apparent phase distribution (thermogram profile). On the other hand, in the case of HSPC:PDMAEMA-b-PLMA 2 9:0.1, the copolymer seemed to promote the most stable phases (high-temperature peak shoulder).

By increasing the copolymer concentration to 9:0.5 (blue curves), the overall effects on the thermodynamic profiles of both the chimeric nanosystems were more pronounced. Indeed, concerning HSPC:PDMAEMA-b-PLMA 1 9:0.5 liposomes, the micro-DSC trace showed an entropic destabilization and a severe phase separation with the presence of two main thermodynamic regions. Such behavior is not necessarily common among chimeric nanosystems, since it has been already reported that polymer insertion in membranes may shift the effective transition to higher temperatures (Pippa et al., 2018). Moreover, the enthalpic contribution to the overall stability became significant, showing a decrease of the transition enthalpy variation to $\Delta H^{\circ} = 33 \pm 2 \text{kJ} \cdot \text{mol}^{-1}$. The enthalpy loss may be explained by considering that the hydrophobic chains constituting the copolymers penetrate into the hydrophobic core of the phospholipid bilayer disturbing the phospholipid-phospholipid interactions and decreasing the amount of lipids contributing to the transition. In the presence of more hydrophobic copolymer chains, that being the case of HSPC:PDMAEMA-b-PLMA 2 9:0.5 vesicles, these effects were amplified. Indeed, the enthalpic contribution to the transition was even lower with this polymer ($\Delta H^{\circ} = 24 \pm 2 \text{ kJ} \cdot \text{mol}^{-1}$). A similar effect has already been observed with DSC analysis on bilayers of these chimeric nanosystems (Naziris et al., 2018).

Regarding the acidic conditions, the two pH-responsive copolymers responded differently and brought about different effects upon the organization of the liposomal membrane, also depending on their molar ratio (**Figure 4**). We have to note that the osmolarity of citrate buffer 100mM is close to that of PBS 150mM, *i.e.* ~300mOsm/L, and as a result, the dilution in these two different media did not affect the osmotic difference between the inner hydration core of liposomes and extravesicular environment, which is important for their thermal behavior (Al-Ayoubi et al., 2018).

HSPC liposomes' thermodynamic profiles exhibited unaltered T_m , narrower $\Delta T_{1/2}$ and higher ΔH° at pH 4.5 compared to those in PBS buffer, revealing stronger phospholipid-phospholipid interaction and higher bilayer compactness. These findings are in line with previously documented results (Koynova and Caffrey, 1998; Naziris et al., 2018).

PDMAEMA-b-PLMA 1 exerted interesting effects on the membrane of chimeric liposomes after exposure to acidic conditions. Namely, both molar ratios led the membrane to a thermodynamic profile that was very close to that of HSPC liposomes, showing the same transition ΔH° , a value that was higher than the respective in PBS, for both 9:0.1 and 9:0.5 preparations. Therefore, differences in the calorimetric traces for these systems between the two media (PBS and citrate buffer) were observed in terms of enrichment of the most stable phase (high-temperature peak), which belongs to pure HSPC liposomes. On the contrary, PDMAEMA-b-PLMA 2 behaved differently. In both 9:0.1 and 9:0.5 molar ratios, the main transition peak slightly shifted towards lower temperatures if compared to the sample in PBS. Moreover, unlike PDMAEMA-b-PLMA 1, an appreciable enthalpy loss was observable by exposing these vesicles in acidic pH, compared with PBS. Therefore, we have two types of pH-responsive effect, depending mainly on the molecular characteristics, composition and hydrophilic-to-hydrophobic balance of the utilized copolymers and not particularly on their concentration inside the chimeric nanosystem. The first comes from a relatively more hydrophilic and pH-responsive but smaller polymer (PDMAEMA-b-PLMA 1), whose effect is probably defined by the pH-responsive segment, transiting the system to the same energy condition with pure membranes. The second however, originates from the relatively more hydrophobic but also larger polymer (PDMAEMA-b-PLMA 2), which has more pH-responsive groups but also a

large hydrophobic segment, which is driven by the pH-responsiveness and through hydrophobic interactions, perturbs the membrane and leads to slight fluidization. The latter effect is probably due to the larger hydrophilic and hydrophobic segments, attributed to the overall greater length of the polymer, where the PDMAEMA block initially becomes more protonated and responds to the lower pH, subsequently affecting the orientation of the PLMA groups inside the HSPC membrane. This evidently caused the deeper penetration of the hydrophobic segments and therefore, the reduction of the transition effectiveness.

In Figure 5, a comparison between two micro-DSC analyses for the HSPC:PDMAEMA-b-PLMA 2 9:0.5 system in PBS is reported, where the second measurement (solid line) was performed a week later than the first one (dashed line). The obtained thermograms were essentially comparable, evidencing the absence of kinetic effects and the achievement of thermodynamic equilibrium for the studied chimeric systems. The same comparison was carried out for all nanosystems, which reproduced the same thermodynamic behavior (data not reported). As a result, despite the differences in enthalpic contribution of the different composition and/or amount of copolymer and final impact on transition enthalpy, all chimeric systems are considered stable and each type of liposome may be utilized in biomedical applications, with potentially divergent biophysical behaviors inside the physiological environment.

To sum up, the phospholipid membrane of the chimeric liposomes was thermotropically affected by the incorporation of amphiphilic copolymers. The transition enthalpy remained the same for the 9:0.1 molar ratio, regardless the type of copolymer, while the higher 9:0.5 polymer ratio resulted in reduced enthalpy, owed to more hydrophobic segments residing inside the membrane. While they were stable in physiological conditions, membranes responded to reduced pH conditions, due to the pH-responsive nature of the polymers.

3.4. In vivo Toxicity of Chimeric Liposomes

HSPC:PDMAEMA-b-PLMA chimeric liposomes were tested for their acute toxicity in immunocompromised male NOD/SCID mice. The four systems were administered intraperitoneally (i.p.) to the mice in a single injection at 400mg/kg or for five days at 200mg/kg, by injecting formulations of 40mg/mL and 20mg/mL respectively (**Table 2**), and their behavior and weight alterations were monitored. HSPC:PDMAEMA-b-PLMA 1 9:0.1 and 9:0.5 caused a slight decrease in mouse weight after administration at 400mg/kg, while this was not observed for 200mg/kg. HSPC:PDMAEMA-b-PLMA 2 9:0.1 and 9:0.5 had no effect at 400mg/kg. All chimeric formulations induced a temporary sedation after administration. These preliminary findings are encouraging for further *in vivo* investigation (Iatrou et al., 2014).

4. Conclusions

The development of DDnSs and especially aDDnSs requires thorough knowledge on the chemical and thermodynamic properties of the biomaterials composing them. The latter, through the self-assembly process, will affect the morphogenesis of new nanostructures, creating innovative properties and functional behavior in the final nanosystem. The nature, the relative and total concentration of the utilized biomaterials and also, the formulation pH, are some very important factors that define self-assembly and their alteration may lead the dynamic lyotropic liquid crystalline system to different morphological and physicochemical characteristics. Based on these features, the fate of pH-responsive chimeric/mixed liposomes inside the

physiological environment will be determined by their interactions with proteins, as well as their behavior in acidic pH conditions. In addition, in order to deliver their final biological stability and effectiveness, these nanoparticles must also be accompanied by the proper biocompatibility and absence of toxicity.

To conclude, formulation parameters, such as the biomaterial concentration, composition and hydration pH, can be optimized to produce quality nanocarrier products, in terms of particle size and polydispersity, while interactions with proteins can be regulated, in order to avoid recognition and excretion before action. All developed nanosystems were evaluated for their physicochemical characteristics in physiological and acidic conditions and their interactions with blood proteins were assessed. Micro-DSC studies on the chimeric liposomes provided insight to the final polymer conformation inside the membrane, with regard to its thermodynamic behavior in different environments. It was shown that these amphiphilic polymers affect the liposomal membrane in a composition- and concentration-dependent manner after incorporation, remain dormant and stable in normal conditions and exhibit functionality in acidic conditions, which is reflected on the thermotropic behavior of liposomes, but not on their physicochemical properties. As a result, thermal analysis is a valuable technique to extract information on the stimuliresponsive behavior of chimeric liposomes. This utility may be exploited for pHresponsive release of drugs or other therapeutic molecules. Preliminary in vivo experiments also indicate the biocompatible nature of these nanosystems and further studies will provide more data on their safety for therapeutic applications.

Acknowledgments

The research work was supported by the Hellenic Foundation for Research and Innovation (HFRI) and the General Secretariat for Research and Technology (GSRT), under the HFRI PhD Fellowship grant (GA. no. 392). The authors also acknowledge the contribution of the PhD student Evangelia Sereti and Associate Professor Konstantinos Dimas, Department of Pharmacology, Faculty of Medicine, School of Health Sciences, University of Thessaly, Greece, for the preliminary *in vivo* results.

Conflict of interest

The authors declare that they have no conflict of interest.

References

Abra RM, Bosworth ME, Hunt CA. Liposome disposition in vivo: effects of predosing with liposomes. Res Commun Chem Pathol Pharmacol. 1980;29(2):349-60.

Akbarzadeh A, Rezaei-Sadabady R, Davaran S, Joo SW, Zarghami N, Hanifehpour Y, Samiei M, Kouhi M, Nejati-Koshki K. Liposome: classification, preparation, and applications. Nanoscale Res Lett. 2013;8(1):102.

Al-Ayoubi SR, Schinkel PKF, Berghaus M, Herzog M, Winter R. Combined effects of osmotic and hydrostatic pressure on multilamellar lipid membranes in the presence of PEG and trehalose. Soft Matter. 2018;14(43):8792-8802.

Anselmo AC, Mitragotri S. Nanoparticles in the clinic. Bioeng Transl Med. 2016;1(1):10-29.

Barenholz Y. Doxil®--the first FDA-approved nano-drug: lessons learned. J Control Release. 2012;160(2):117-134.

Barone G, Del Vecchio P, Fessas D, Giancola C, Graziano G. THESEUS: A new software package for the handling and analysis of thermal denaturation data of biological macromolecules. Journal of Thermal Analysis. 1992;38(12):2779-2790.

Baughman RH, Zakhidov, AA, de Heer WA. Carbon Nanotubes – The Route toward Applications. Science 2002;297(5582):787-792.

Bharti C, Nagaich U, Pal AK, Gulati N. Mesoporous silica nanoparticles in target drug delivery system: A review. Int J Pharm Investig. 2015;5(3):124-133.

Böhme U, Scheler U. Effective charge of bovine serum albumin determined by electrophoresis NMR. Chem Phys Letters. 2007;435(4-6):342-345.

Bulbake U, Doppalapudi S, Kommineni N, Khan W. Liposomal Formulations in Clinical Use: An Updated Review. Pharmaceutics. 2017;9(2).

Chrysostomou V, Pispas S. Stimuli-responsive amphiphilic PDMAEMA-b-PLMA copolymers and their cationic and zwitterionic analogs. J Polym Sci A Polym Chem. 2018;56(6):598-610.

Colombo M, Carregal-Romero S, Casula MF, Gutiérrez L, Morales MP, Böhm IB, Heverhagen JT, Prosperi D, Parak WJ. Biological applications of magnetic nanoparticles. Chem Soc Rev. 2012;41(11):4306-4334.

Danhier F, Feron O, Preat V. To exploit the tumor microenvironment: passive and active tumor targeting of nanocarriers for anti-cancer drug delivery. J Control Release 2010;148(2):135-146.

Demetzos C, Pippa N. Advanced drug delivery nanosystems (aDDnSs): a minireview. Drug Deliv. 2014;21(4):250-257.

Deshpande PP, Biswas S, Torchilin VP. Current trends in the use of liposomes for tumor targeting. Nanomedicine (Lond). 2013;8(9):1509-1528.

Doherty GJ, McMahon HT. Mechanisms of endocytosis. Annu Rev Biochem 2009;78:857-902.

Eloy JO, Claro de Souza M, Petrilli R, Barcellos JP, Lee RJ, Marchetti JM. Liposomes as carriers of hydrophilic small molecule drugs: strategies to enhance encapsulation and delivery. Colloids Surf B Biointerfaces. 2014;123:345-363.

Felber AE, Dufresne MH, Leroux JC. pH-sensitive vesicles, polymeric micelles, and nanospheres prepared with polycarboxylates. Adv Drug Deliv Rev. 2012;64(11):979-992.

Frankel AD, Pabo CO. Cellular uptake of the tat protein from human immunodeficiency virus. Cell 1988;55(6):1189-1193.

Gardikis K, Hatziantoniou S, Signorelli M, Pusceddu, Micha-Screttas M, Schiraldi A, Demetzos C, Fessas D. Thermodynamic and structural characterization of Liposomal-Locked in-Dendrimers as drug carriers. Colloids Surfaces B Biointerfaces. 2010;81(1):11-19.

Günther M, Lipka J, Malek A, Gutsch D, Kreyling W, Aigner A. Polyethylenimines for RNAi-mediated gene targeting in vivo and siRNA delivery to the lung. Eur J Pharm Biopharm 2011;77(3):438-449.

Iatrou H, Dimas K, Gkikas M, Tsimblouli C, Sofianopoulou S. Polymersomes from polypeptide containing triblock Co- and terpolymers for drug delivery against pancreatic cancer: asymmetry of the external hydrophilic blocks. Macromolecular Bioscience. 2014;14(9):1222-1238.

Kanamala M, Wilson WR, Yang M, Palmer BD, Wu Z. Mechanisms and biomaterials in pH-responsive tumour targeted drug delivery: A review. Biomaterials. 2016;85:152-167.

Kitayama H, Takechi Y, Tamai N, Matsuki H, Yomota C, Saito H. Thermotropic phase behavior of hydrogenated soybean phosphatidylcholine-cholesterol binary liposome membrane. Chem Pharm Bull (Tokyo). 2014;62(1):58-63.

Knudsen KB, Northeved H, Kumar PE, Permin A, Gjetting T, Andresen TL, Larsen S, Wegener KM, Lykkesfeldt J, Jantzen K, Loft S, Møller P, Roursgaard M. In vivo toxicity of cationic micelles and liposomes. Nanomedicine. 2015;11(2):467-77.

Koynova R, Caffrey M. Phases and phase transitions of the phosphatidylcholines. Biochim Biophys Acta. 1998;1376(1):91-145.

Lehner R, Wang X, Marsch S, Hunziker P. Intelligent nanomaterials for medicine: carrier platforms and targeting strategies in the context of clinical application. Nanomedicine. 2013;9(6):742-757.

Lin CA, Yang TY, Lee CH, Huang SH, Sperling RA, Zanella M, Li JK, Shen JL, Wang HH, Yeh HI, Parak WJ, Chang WH. Synthesis, characterization, and bioconjugation of fluorescent gold nanoclusters toward biological labeling applications. ACS Nano. 2009;3(2):395-401.

Maeda H. The enhanced permeability and retention (EPR) effect in tumor vasculature: the key role of tumor-selective macromolecular drug targeting. Adv Enzyme Regul, 2001;41(1):189-207.

Mohr K, Müller SS, Müller LK, Rusitzka K, Gietzen S, Frey H, Schmidt M. Evaluation of multifunctional liposomes in human blood serum by light scattering. Langmuir. 2014;30(49):14954-1462.

Naziris N, Pippa N, Chrysostomou V, Pispas S, Demetzos C, Libera M, et al. Morphological diversity of block copolymer/lipid chimeric nanostructures. J Nanopart Res. 2017;19(10):347-357.

Naziris N, Pippa N, Pispas S, Demetzos C. Stimuli-responsive drug delivery nanosystems: from bench to clinic. Curr Nanomed. 2016;6(3):1-20.

Naziris N, Pippa N, Stellas D, Chrysostomou V, Pispas S, Demetzos C, Libera M, Trzebicka B. Development and Evaluation of Stimuli-Responsive Chimeric Nanostructures. AAPS PharmSciTecq. 2018;19(7):2971-2989.

National Cancer Institute. 2015.

https://dtp.cancer.gov/organization/btb/acute_toxicity.htm [ONLINE] Available at: https://www.cancer.gov/. [Accessed 4 July 2019].

Nurunnabi M, Khatun Z, Reeck GR, Lee DY, Lee YK. Photoluminescent graphene nanoparticles for cancer phototherapy and imaging. ACS Appl Mater Interfaces. 2014;6(15):12413-12421.

Palchetti S, Caputo D, Digiacomo L, Capriotti AL, Coppola R, Pozzi D, Caracciolo G. Protein Corona Fingerprints of Liposomes: New Opportunities for Targeted Drug Delivery and Early Detection in Pancreatic Cancer. Pharmaceutics. 2019;11(1). pii: E31.

Palchetti S, Colapicchioni V, Digiacomo L, Caracciolo G, Pozzi D, Capriotti AL, La Barbera G, Laganà A. The protein corona of circulating PEGylated liposomes. Biochimica et Biophysica Acta. 2016a;1858(2):189-196.

Palchetti S, Digiacomo L, Pozzi D, Peruzzi G, Micarelli E, Mahmoudi M, Caracciolo G. Nanoparticles-cell association predicted by protein corona fingerprints. Nanoscale. 2016b;8(25):1275

Palmerston Mendes L, Pan J, Torchilin VP. Dendrimers as Nanocarriers for Nucleic Acid and Drug Delivery in Cancer Therapy. Molecules. 2017;22(9):1401.

Papageorgiou F, Pippa N, Naziris N, Demetzos C. Physicochemical Study of the Protein-Liposome Interactions: Influence of Liposome Composition and Concentration on Protein Binding. J Liposome Res. 2018, Epub ahead of print.

Parak WJ, Pellegrino T, Plank C. Labelling of cells with quantum dots. Nanotechnology. 2005;16(2):R9-R25.

Pelaz B, Alexiou C, Alvarez-Puebla RA, Alves F, et al. Diverse Applications of Nanomedicine. ACS Nano. 2017;11(3):2313-2381.

Pippa N, Deli E, Mentzali E, Pispas S, Demetzos C. PEO-b-PCL grafted DPPC liposomes: physicochemical characterization and stability studies of novel bio-inspired advanced drug delivery nano systems (aDDnSs). J Nanosci Nanotechnol. 2014;14:5676-5681.

Pippa N, Perinelli DR, Stergios P, Bonacucina G, Demetzos C, Forys A, Trzebicka B. Studying the colloidal behavior of chimeric liposomes by cryo-TEM, microdifferential scanning calorimetry and high-resolution ultrasound spectroscopy. Colloids and Surfaces A: Physicochemical and Engineering Aspects. 2018;555:539-547.

Pippa N, Stellas D, Skandalis A, Pispas S, Demetzos C, Libera M, Marcinkowski A, Trzebicka B. Chimeric lipid/block copolymer nanovesicles: Physico-chemical and bio-compatibility evaluation. Eur J Pharm Biopharm. 2016;107:295-309.

Saitta F, Signorelli M, Fessas D. Dissecting the effects of free fatty acids on the thermodynamic stability of complex model membranes mimicking insulin secretory granules. Colloids Surf B Biointerfaces. 2019;176:167-175.

Samsonova O, Pfeiffer C, Hellmund M, Merkel OM, Kissel T. Low molecular weight pDMAEMA-block-pHEMA blockcopolymers synthesized via RAFT-polymerization: potential non-viral gene delivery agents? Polymer. 2011;3(2):693-718.

Schellekens H, Stegemann S, Weinstein V, de Vlieger JS, Flühmann B, Mühlebach S, Gaspar R, Shah VP, Crommelin DJ. How to regulate nonbiological complex drugs (NBCD) and their follow-on versions: points to consider. AAPS J, 2014;16(1):15-21.

Schulz M, Binder WH. Mixed Hybrid Lipid/Polymer Vesicles as a Novel Membrane Platform. Macromol Rapid Commun. 2015;36(23):2031-2041.

Torchilin VP. Micellar Nanocarriers: Pharmaceutical Perspectives. Pharm Res. 2007;24(1):1-16.

Tribet C, Vial F. Flexible macromolecules attached to lipid bilayers: impact on fluidity, curvature, permeability and stability of the membranes. Soft Matter. 2008;4:68-81.

Wei X, Cohen R, Barenholz Y. Insights into composition/structure/function relationships of Doxil® gained from "high-sensitivity" differential scanning calorimetry. Eur J Pharm Biopharm. 2016;104:260-270.

Xiao-ying Zhang, Pei-ying Zhang. Polymersomes in Nanomedicine - A Review. Curr Med Chem. 2017;13(2):124-129.

Yu SJ, Kang MW, Chang HC, Chen KM, Yu YC. Bright fluorescent nanodiamonds: no photobleaching and low cytotoxicity. J Am Chem Soc. 2005;127(50):17604-17605.

Zeitlinger MA, Derendorf H, Mouton JW, Cars O, Craig WA, Andes D, Theuretzbacher U. Protein binding: do we ever learn? Antimicrob Agents Chemother. 2011;55(7):3067-3074.

Zengin A, Karakose G, Caykara T. Poly(2-(dimethylamino)ethyl methacrylate) brushes fabricated by surface-mediated RAFT polymerization and their response to pH. Eur Polym J. 2013;49(10):3350-3358.

Zhang R, Yang J, Sima M, Zhou Y, Kopeček J. Sequential Combination Therapy of Ovarian Cancer with Degradable N-(2-hydroxypropyl)methacrylamide Copolymer Paclitaxel and Gemcitabine Conjugates. Proc Natl Acad Sci USA. 2014;111(33):12181-12186.

Zhu C, Jung S, Luo S, Meng F, Zhu X, Park TG, Zhong Z. Co-delivery of siRNA and paclitaxel into cancer cells by biodegradable cationic micelles based on PDMAEMA-PCL-PDMAEMA triblock copolymers. Biomaterials. 2010;31(8):2408-16.

Figure 1: Molecular structures of A. HSPC, B. PDMAEMA-b-PLMA and C. Self-assembled supramolecular structure of the two biomaterials.

Figure 2: Cryo-TEM images of A. HSPC:PDMAEMA-b-PLMA 1 9:0.1, B. HSPC:PDMAEMA-b-PLMA 1 9:0.5, C. HSPC:PDMAEMA-b-PLMA 2 9:0.1 and D. HSPC:PDMAEMA-b-PLMA 2 9:0.5

Figure 3: DSC heating scans for HSPC bilayers/MLVs (blue) and liposomes/SUVs (black) in PBS.

Figure 4: Micro-DSC scans for HSPC (black), HSPC:PDMAEMA-b-PLMA 1 9:0.1 (red) and 9:0.5 (blue) in PBS (top) and citrate buffer (bottom) and HSPC (black), HSPC:PDMAEMA-b-PLMA 2 9:0.1 (red) and 9:0.5 (blue) chimeric liposomes in PBS (top) and citrate buffer (bottom). Heating and cooling curves are shown as solid and dashed lines, respectively (reference cooling curve not shown).

Figure 5: Micro-DSC heating scans for HSPC:PDMAEMA-*b*-PLMA 2 9:0.5 on the first day (dashed line) and after a week (solid line).

Table 1: Physicochemical characteristics of HSPC:PDMAEMA-b-PLMA 1 and HSPC:PDMAEMA-b-PLMA 2 chimeric systems of biomaterial concentration 5mg/mL that were utilized in the micro-DSC experiments, in PBS (pH 7.0), acidic environment (citrate buffer, pH 4.5) and FBS.

System	Molar Ratio	Dispersion Medium	D _h ¹ (nm)	SD ²	PDI ³	SD ²	Z-pot ⁴ (mV)	SD ²
HSPC Liposomes	-	PBS (pH=7.0)	113.4	1.9	0.509	0.015	2.2	0.6
		Citrate Buf. (pH=4.5)	115.6	2.4	0.487	0.010	0.0	1.3
		FBS	Aggr ⁵	Aggr ⁵	Aggr ⁵	Aggr ⁵	-	-

ournal	Pre-pro	ofe
oumai	110-010	012

	9:0.1	PBS (pH=7.0)	82.9	0.7	0.281	0.021	11.5	4.3
		Citrate Buf. (pH=4.5)	85.7	0.6	0.308	0.002	18.6	2.6
HSPC:		FBS	189.1	1.6	1.000	0.000		
PDMAEMA-b-PLMA 1	9:0.5	PBS (pH=7.0)	83.1	0.9	0.233	0.003	14.4	1.9
		Citrate Buf. (pH=4.5)	82.4	0.5	0.269	0.004	20.6	3.3
		FBS	183.6	3.0	1.000	0.000	-	-
		PBS (pH=7.0)	75.4	0.7	0.253	0.025	15.6	2.2
	9:0.1	Citrate Buf. (pH=4.5)	80.9	0.2	0.328	0.009	18.6	1.4
HSPC:		FBS	165.3	2.4	1.000	0.000	-	-
PDMAEMA-b-PLMA 2		PBS (pH=7.0)	83.3	0.7	0.209	0.008	15.8	1.7
	9:0.5	Citrate Buf. (pH=4.5)	81.7	0.6	0.239	0.011	19.3	2.4
		FBS	126.6	2.5	0.867	0.011	-	-

¹Hydrodynamic diameter

²Standard deviation

³Polydispersity index

⁴Zeta potential

⁵Aggregate Formation

Table 2: Physicochemical characteristics of HSPC:PDMAEMA-b-PLMA 1 and HSPC:PDMAEMA-b-PLMA 2 chimeric systems that were utilized in the *in vivo* experiments in PBS.

System	Molar Ratio	Biomaterial Concentration	Dispersion Medium	D _h ¹ (nm)	SD ²	PDI ³	SD ²	Z-pot ⁴ (mV)	SD ²	
HSPC:	9:0.1		PBS	120.3	1.0	0.298	0.008	36.0	2.2	
PDMAEMA-b-PLMA 1	9:0.5	40mg/mL	10	(pH=7.4)	119.6	1.1	0.256	0.013	14.9	3.6
HSPC:	9:0.1		PBS	121.3	1.0	0.491	0,010	24.6	0.4	
PDMAEMA-b-PLMA 2	9:0.5		(pH=7.4)	97.5	0.5	0.254	0,007	14.3	3.0	
HSPC:	9:0.1	20m ~/m I	PBS	139.9	0.5	0.408	0,007	41.0	0.4	
PDMAEMA-b-PLMA 1	9:0.5	20mg/mL	(pH=7.4)	67.9	0.6	0.191	0,014	13.3	0.5	

HSPC:	9:0.1	PBS	97.0	0.9	0.293	0,002	26.6	2.3
PDMAEMA-b-PLMA 2	9:0.5	(pH=7.4)	82.9	0.3	0.255	0,012	13.2	2.2

¹Hydrodynamic diameter

²Standard deviation

³Polydispersity index

⁴Zeta potential

Table 3: Thermodynamic parameters, evaluated from micro-DSC investigations and

obtained by considering the second heating-cooling cycle.

	Malar		Main Transition				Pre-transition		
System	Molar Ratio	рН	ΔH° (kJ·mol ⁻¹)	T _{m,1} ^{app} (°C)	T _{m,2} app (°C)	$\Delta_r T_{1/2}$	ΔH° (kJ·mol ⁻¹)	T _p ^{app} (°C)	
HSPC MLVs	-	7.0	40 ± 2	53.8 ± 0.1	-	1.0 ± 0.1	3 ± 1	48.2 ± 0.1	
HSPC Liposomes	-	7.0	40 ± 2	52.2 ± 0.1	53.5 ± 0.2	4.4 ± 0.1	-	-	
		4.5	46 ± 2	52.4 ± 0.1	53.1 ± 0.2	4.4 ± 0.1	-	-	
	9:0.1	7.0	40 ± 2	53.6 ± 0.1	55.3 ± 0.2	5.2 ± 0.1	-	-	
HSPC:		4.5	46 ± 2	53.4 ± 0.2	-	4.5 ± 0.1	-	-	
PDMAEMA-b-PLMA 1	9:0.5	7.0	33 ± 2	51.4 ± 0.1	53.5 ± 0.1	7.5 ± 0.1	-	-	
		4.5	45 ± 2	52.4 ± 0.2	53.0 ± 0.1	5.1 ± 0.1	-	-	
	9:0.1	7.0	40 ± 2	52.5 ± 0.2	54.1 ± 0.1	4.8 ± 0.1	-	-	
HSPC: PDMAEMA-b-PLMA 2		4.5	37 ± 2	52.6 ± 0.2	53.4 ± 0.1	4.5 ± 0.1	-	-	
	9:0.5	7.0	24 ± 2	52.7 ± 0.2	53.7 ± 0.1	4.6 ± 0.1	-	-	
		4.5	23 ± 2	53.2 ± 0.2	-	4.7 ± 0.1	-	-	